



Cite this: DOI: 10.1039/c9nj05273a

# Construction of a tandem HZSM-5 with CuZnAl catalyst for alkylation of benzene with syngas†

 Bize Gao,<sup>a</sup> Chuanmin Ding,<sup>ib</sup>\*<sup>a</sup> Junwen Wang,<sup>ib</sup><sup>a</sup> Guangyue Ding,<sup>a</sup> Jinxiang Dong,<sup>ib</sup><sup>a</sup> Hui Ge\*<sup>b</sup> and Xuekuan Li<sup>b</sup>

Aiming at the problem of over-production of benzene and the demand for aromatics in industry, a CuO/ZnO/Al<sub>2</sub>O<sub>3</sub> catalyst was prepared by a coprecipitation method, and mixed with ZSM-5 to form a bifunctional composite catalyst. The prepared catalyst is used in an alkylation reaction of benzene with synthesis gas in a liquid phase in a slurry bed reactor. A series of analytical methods such as ammonia gas temperature programmed desorption (NH<sub>3</sub>-TPD), X-ray diffraction (XRD), nitrogen adsorption-desorption, scanning electron microscopy (SEM) and inductively coupled plasma emission spectrometry (ICP) were conducted to characterize the catalyst. The results show that the structure and acidity of the modified ZSM-5 have changed during the modification process, and ZSM-5 produces a more mesoporous structure after desilicization. Therefore, the specific surface area of the modified ZSM-5 zeolite increases and the number of acid sites become smaller than those of the unmodified zeolite. The results show that the acid-modified ZSM-5 improves the conversion of CO, while the selectivity of CO to aromatics decreases. In contrast, only alkali modification and acid-alkali co-modification on ZSM-5 contributed to increasing the selectivity to aromatics, especially acid-alkali co-modified ZSM-5. The reason for this can be attributed to the fact that the modified zeolite produces a mesoporous structure, enhancing the mass transfer ability further. Moreover, the amount of strong acid sites on the modified ZSM-5 is reduced, which reduces the side reaction of methanol and olefin, thereby improving the selectivity of CO to aromatics.

 Received 21st October 2019,  
 Accepted 12th December 2019

DOI: 10.1039/c9nj05273a

[rsc.li/njc](http://rsc.li/njc)

## 1. Introduction

Aromatic hydrocarbons are the most important basic organic compounds in the petrochemical industry. Among aromatic hydrocarbons, *para*-xylene (PX) is the most valuable xylene isomer, which can be converted into PET (polyethylene terephthalate), fibers, films, resins, PBT (polybutylene terephthalate) and other chemical compounds.<sup>1–3</sup> Although there are many reports on the preparation of aromatic hydrocarbons by alkylation of benzene, they are still limited to small-scale production. The source of benzene is very extensive and can be obtained by petroleum processing, coal tar processing, alkane aromatization, catalytic reforming, and aromatics-separation. With the continuous improvement of industrial systems, the production capacity of benzene has continued to increase in recent years with a situation of overproduction.<sup>4,5</sup> Therefore, the comprehensive

utilization of benzene has become an urgent problem to be solved. Traditional preparation methods of aromatic hydrocarbons include methanol to aromatic hydrocarbons, toluene alkylation to produce xylene and so on, but the scale in actual production is small. Syngas composed of hydrogen and carbon monoxide can be produced from non-petroleum carbon resources such as coal, natural gas and biomass, which are cheap and easy to obtain, and has been widely used in industrial production, and has attracted great attention. Therefore, it is more economical to prepare aromatic hydrocarbons by alkylation of excess produced benzene with syngas than by traditional methods.<sup>6,7</sup>

ZSM-5 zeolite is widely used in the alkylation reaction of benzene with methanol due to its special surface area, adjustable acidity and unique pore structure.<sup>8–11</sup> Furthermore, due to its high selectivity, activity and stability, HZSM-5 has been widely used for the aromatization of methanol.<sup>12–14</sup> The CuO/ZnO/Al<sub>2</sub>O<sub>3</sub> catalyst is well-acknowledged for syngas to methanol reaction.<sup>15,16</sup> The reaction of benzene with syngas could be considered as coupling of syngas conversion to methanol and reaction of benzene with the methanol to form toluene. In recent years, the idea of constructing a multifunctional composite catalyst for continuous reaction has been extensively studied.<sup>17,18</sup> For instance, Jiao *et al.*<sup>18</sup> used ZnCrOx + MSAPO as a bifunctional

<sup>a</sup> College of Chemistry & Chemical Engineering, Taiyuan University of Technology, Taiyuan 030024, P. R. China. E-mail: dingchuanmin@tyut.edu.cn, wangjunwen@tyut.edu.cn; Fax: +86-0351-6014498

<sup>b</sup> State Key Laboratory of Coal Conversion, Institute of Coal Chemistry of CAS, Taiyuan 030001, China. E-mail: gehui@sxicc.ac.cn

† Electronic supplementary information (ESI) available. See DOI: 10.1039/c9nj05273a

composite catalyst for the conversion of synthesis gas to light olefins. If ZSM-5 and CuO/ZnO/Al<sub>2</sub>O<sub>3</sub> are mixed, a bifunctional composite catalyst having catalytic hydrogenation and alkylation sites can be prepared.<sup>19–21</sup> Previous research on alkylation of benzene with syngas using bifunctional composite catalysts has been very rare. Therefore, the design and construction of high-efficiency catalysts for the alkylation of benzene with syngas is of great significance.

Mass transfer capacity is a very important property of the catalyst, because the mobility of the molecule in the catalyst will ultimately determine the rate of desorption and catalytic reaction.<sup>22–24</sup> However, the inherent microporous structure in conventional ZSM-5 inhibits the mass transfer capacity of ZSM-5, which results in a very low selectivity to toluene and xylene for in the benzene alkylation.<sup>25</sup> In order to solve the problem of catalyst mass transfer and deactivation in the catalytic reaction, larger size pores, like mesopores, are usually introduced into the zeolite to improve the mass transfer ability of the catalyst, and thus improve the contact between the active sites of the catalyst and the reactant molecules.<sup>24,26</sup> Common methods for the preparation of mesopores include limiting crystal growth,<sup>27</sup> introduction of a carbon template or polymeric mesoporous template<sup>28,29</sup> and post-synthesis dealumination or desilicization.<sup>30</sup> The first two types of methods are very expensive and can be harmful to the environment.<sup>31</sup> However, dealumination or desilicization of zeolite by acid or alkali modification has proved to be a simple and low-cost pathway and can significantly increase the production of aromatics.<sup>31–34</sup> Bjørgen *et al.*<sup>35</sup> studied the effect of desilicization of ZSM-5 on the MTG reaction and discovered that the alkali modified ZSM-5 improved the selectivity to the product in the MTG reaction. Li *et al.*<sup>36</sup> studied the effect of desilicization of ZSM-5 on its catalytic performance in the catalytic pyrolysis of lignocellulosic biomass and found that the desilicized ZSM-5 formed many mesopores, and the diffusion properties of ZSM-5 were also improved, and more aromatic hydrocarbons are also produced in the reaction product.

In addition to improving the mass transfer capacity, acid and alkali modification can remove the aluminum element and the silicon element in the ZSM-5, regulating acid strength and density and adjusting the catalytic performance further.<sup>35,37–40</sup> Meng *et al.*<sup>41</sup> modified ZSM-5 with HF and used it in the MTG reaction, indicating that the acid content of the zeolite treated with HF changed significantly and many mesoporous structures were formed at the same time, and the conversion rate of methanol was also significantly improved. Mochizuki *et al.*<sup>42</sup> used NaOH to desilicize HZSM-5 zeolite for the hexane cracking reaction, and studied the influence of the outer surface and acidity on its catalytic performance in hexane cracking, and the results showed that NaOH modification regulated the acid content of HZSM-5 and reduced the production of coke.

In this study, a series of ZSM-5 molecular sieves were prepared by desilicization and dealumination of ZSM-5 molecular sieves by sodium hydroxide and oxalic acid, respectively, and then combined with Cu/ZnO/Al<sub>2</sub>O<sub>3</sub> to form a bifunctional composite catalyst for alkylation of benzene with syngas. Besides, this study

was conducted using a slurry bed instead of the traditional fixed bed. This study focuses on the construction of a tandem catalyst and the effects of changing morphology and acid property of the tandem catalyst on the alkylation of benzene in homogeneous reaction systems.

## 2. Experimental

### 2.1 Preparation of CuO/ZnO/Al<sub>2</sub>O<sub>3</sub>

The CuO/ZnO/Al<sub>2</sub>O<sub>3</sub> catalyst was prepared by a co-precipitation method. 14.86 g Cu(NO<sub>3</sub>)<sub>2</sub>, 8.92 g Zn(NO<sub>3</sub>)<sub>2</sub> and 3.75 g Al(NO<sub>3</sub>)<sub>3</sub> were weighed and dissolved in 200 ml distilled water to make a mixed nitrate solution of copper, zinc and aluminum ( $n(\text{Cu}):n(\text{Zn}):n(\text{Al}) = 6:3:1$ ). Then, 11.50 g Na<sub>2</sub>CO<sub>3</sub> was dissolved in 200 ml of distilled water, and the concentration was set to 1 mol L<sup>-1</sup> to prepare an alkali solution; 100 ml of distilled water was added to a beaker having a capacity of 500 ml, and the beaker was placed in a water bath which had been raised to 80 °C; the mixed solution and the alkali solution were slowly dropped into the beaker. The precipitate was heated to 80 °C in a water bath; the precipitate was aged for 2 h, while maintaining a water bath temperature of 80 °C. After the aging was completed, the precipitate was suction filtered and washed with distilled water and ethanol. After drying at 110 °C for 12 hours, a precursor of the catalyst was obtained. The precursor was placed in a muffle furnace and calcined at 550 °C for 4 h to obtain the final CuO/ZnO/Al<sub>2</sub>O<sub>3</sub> catalyst.

### 2.2 Preparation of HZSM-5 and modified HZSM-5

The HZSM-5 and modified HZSM-5 precursors were prepared using a modification of the method reported in the literature.<sup>43</sup> Commercial ZSM-5 (Nankai Chemical Plant, NH<sub>4</sub> form) with an Si/Al ratio of 150 was used in this experiment. Before use, the zeolite was calcined in air at 550 °C for 7 hours to obtain ZSM-5.

10 g of the zeolite and 100 ml of a 1 mol L<sup>-1</sup> oxalic acid solution were placed in a round bottom flask, and stirred at 363 K for 2 hours under stirring and reflux. Then, the solid was filtered and washed repeatedly with distilled water until the acid was completely removed. Finally, the sample was dried at 383 K and calcined at 823 K for 7 hours to obtain an acid-modified zeolite, designated ZSM-5-H.

In the same manner, ZSM-5 was suspended in a 0.5 mol L<sup>-1</sup> NaOH solution at 353 K for 2 hours under stirring and reflux to produce a mixture. The mixture was then immediately cooled and then washed with deionized water. Finally, the prepared zeolite sample was dried overnight at 383 K, then exchanged three times in 0.5 mol L<sup>-1</sup> NH<sub>4</sub>Cl solution, and calcined in air at 823 K for 7 hours to produce an alkali-modified zeolite, labeled as ZSM-5-OH. Acid-alkali co-modified zeolite is represented by ZSM-5-H-OH.

### 2.3 Catalyst characterization

X-ray diffraction (XRD) of the catalyst was carried out using a SHIMADZU-6000 X-ray powder diffractometer (Shimadzu, Japan). The crystal form and crystallinity of the catalyst were analyzed. The copper target K $\alpha$  radiation was 2 kW and the

scanning range was 5–85°. The scanning speed is 8° min<sup>-1</sup>. NH<sub>3</sub> temperature programmed desorption (TPD) of the catalysts was carried out using a Tianjin XQ TP-5076 chemisorption instrument equipped with a thermal conductivity detector (TCD). Transmission electron microscopy (TEM) images were taken on FEI F30 transmission electron microscopes. The overall composition of the catalyst (Si/Al and Si/Zn) was analyzed using an ICP-AES Autoscan 16 inductively coupled plasma optical emission spectrometer (TJA, USA). The specific surface area, pore volume and pore size of the molecular sieve catalyst were analyzed using a BELSORP-max type surface adsorber (McKerker). The catalyst was first treated under high vacuum (<10<sup>-4</sup> Torr) and 400 °C for 6 h before testing to remove the impurities on the surface of the molecular sieve and the adsorption in the pores. Specifically, the specific surface area was calculated by the BET method; the micropore volume was measured by the *t*-plot method, and the mesoporous volume was measured by the BJH method.

## 2.4 Catalyst testing

The prepared CuO/ZnO/Al<sub>2</sub>O<sub>3</sub> and ZSM-5 were ground and mixed in a ratio of 1:1. Prior to the reaction, the catalyst was reduced with hydrogen at 250 °C for 4 h. 2 g of the catalyst and 20 ml of benzene were added to the slurry bed reactor, and syngas was introduced at a certain temperature and pressure for 8 hours. The product was cooled by condensed water and analyzed by gas chromatography.

The conversion of CO (*C*), selectivity of CO to toluene (*S<sub>T</sub>*), selectivity of CO to ethylbenzene (*S<sub>EB</sub>*), selectivity of CO to xylene (*S<sub>X</sub>*) and selectivity of carbon monoxide to *para*-xylene (*S<sub>PX</sub>*) are defined as follows, respectively:

$$C(\%) = \frac{\text{CO in feed} - \text{CO in product}}{\text{CO in feed}}$$

$$S_T(\%) = \frac{n(\text{the amount of CO converted to toluene})}{n(\text{conversion of CO})}$$

$$S_X(\%) = \frac{n(\text{the amount of CO converted to xylene})}{n(\text{conversion of CO})}$$

$$S_{EB}(\%) = \frac{n(\text{the amount of CO converted to EB})}{n(\text{conversion of CO})}$$

$$S_{PX}(\%) = \frac{n(\text{the amount of CO converted to } para\text{-xylene})}{n(\text{conversion of CO})}$$

## 3. Results and discussion

### 3.1 Catalyst characterization

The parent ZSM-5 is treated with acid and alkali for 2 h, thereby removing aluminum and silicon atoms on the molecular sieve framework, and introducing a mesoporous structure into the ZSM-5 zeolite. The obtained ZSM-5 and Cu/ZnO/Al<sub>2</sub>O<sub>3</sub> were mixed at a ratio of 1:1 to form a bifunctional composite

catalyst, which was employed in the alkylation reaction of benzene with syngas in a slurry bed reactor. This study focuses on the effects of acid-treatment, base-treatment, and acid-alkali co-treatment on the catalytic performance of alkylation of benzene with syngas.

The powder XRD patterns of these four samples are shown in Fig. 6. All the samples demonstrated characteristic peaks of an MFI crystal structure between 7–10° and 22–25°,<sup>44,45</sup> and all of the samples show the skeleton structure of ZSM-5 and have good crystallinity. However, the intensity of the peaks has changed significantly. The crystallinity of the acid-modified ZSM-5 is slightly increased, while the crystallinity of the alkali-modified ZSM-5 is slightly reduced due to the formation of an amorphous phase.<sup>46</sup> This suggests that desilicization occurred under alkali treatment. At the time of aging of the gel, the degree of crystallinity slightly increased (ZSM-5-H), suggesting that dealumination in the zeolite framework was negligible. Fig. S1 (ESI†) is an XRD spectrum of a different catalyst before mixing with ZSM-5. It can be found from Fig. S1 (ESI†) that the diffraction peaks of CuO and ZnO alone are more obvious, and the crystallinity is better. The diffraction peaks of CuO and ZnO also can be seen in the graph of CuO/ZnO/Al<sub>2</sub>O<sub>3</sub>, but they are more diffuse than a and b. It shows that as the composition increases, the crystallinity deteriorates and the dispersibility is better.

As shown in Fig. 2, the ZSM-5 structure changed during the modification process. The peak with a desorption temperature between 200 and 250 °C represents a weak acid level; the peak with a desorption temperature between 300 and 450 °C represents a medium acid level; the peak with desorption temperature between 600 and 800 °C represents a strong acid level. It is mainly caused by the desorption of NH<sub>3</sub> adsorbed on the strong acid sites of molecular sieves. In general, the area of the NH<sub>3</sub> desorption peak can be used to measure the amount of acidity of the molecular sieve.<sup>47</sup> Table 1 summarizes the acidity of these zeolites. The acidity of ZSM-5 is an important factor in determining the catalytic activity and product selectivity of the alkylation reaction of benzene. It is well known that the amount of ammonia desorbed from the catalyst surface can be estimated at the peak temperature, by the TPD peak area and acid strength properties. It was observed that the modified sample exhibited varying degrees of change in the number and intensity of acid sites compared to unmodified ZSM-5. The alkali-modified ZSM-5 had greatly reduced strong acid sites, while the weak acid and medium acid sites were

Table 1 Acid content and distribution of different ZSM-5

Samples <sup>a</sup>	Acid sites <sup>b</sup> /(mmol g <sup>-1</sup> )			Total acidity
	Weak acidity	Medium acidity	Strong acidity	
ZSM-5	0.037	0.108	0.223	0.368
ZSM-5-H	0.069	0.110	0.284	0.219
ZSM-5-OH	0.093	0.123	0.003	0.463
ZSM-5-H-OH	0.049	0.098	0.032	0.179

<sup>a</sup> *m*<sub>cat</sub> = 0.1 g. <sup>b</sup> Density of acid sites, determined by NH<sub>3</sub>-TPD (total: NH<sub>3</sub> desorbed at 200–800 °C; strong: NH<sub>3</sub> desorbed at 600–800 °C).

Table 2 Silicon to aluminum ratio of different ZSM-5

Samples	Composition (ICP-AES)		
	Si/mg L <sup>-1</sup>	Al/mg L <sup>-1</sup>	SiO <sub>2</sub> /Al <sub>2</sub> O <sub>3</sub>
ZSM-5	40.69	0.54	150.70
ZSM-5-H	42.32	0.51	165.96
ZSM-5-OH	40.29	0.88	91.57
ZSM-5-H-OH	38.79	0.55	141.05

significantly increased. The number of weak acid sites on the acid-modified ZSM-5 increased slightly, the medium acid sites were almost unchanged, and the strong acid sites increased slightly. The ZSM-5 modified by acid and alkali also showed a significant decrease in the strong acid sites, the weak acid sites increased slightly, and the medium and strong acid sites decreased slightly. This indicates that the alkali modification has a significant effect on the strong acid sites of ZSM-5, and the acid modification has a significant effect on the weak acid sites of ZSM-5. From the above studies we conclude that alkali or acid modification further modulates the acid properties of the ZSM-5 zeolite.

Table 2 shows the results of elemental analysis of different ZSM-5 ICP-AES measurements. We can find that the unmodified ZSM-5 has a ratio of SiO<sub>2</sub>/Al<sub>2</sub>O<sub>3</sub> of 150 (nominal SiO<sub>2</sub>/Al<sub>2</sub>O<sub>3</sub> ratio of 150); the acid-modified ZSM-5 is increased to 165.96 (ZSM-5-H), the alkali-modified ZSM-5 is reduced to 91.57 (ZSM-5-OH), and the acid-alkali co-modified ZSM-5 is reduced to 150.7 (ZSM-5-H-OH). This change indicates that part of the framework of the acid and base modification-processed ZSM-5 dissolves, thereby achieving the purpose of desilicization and dealumination.<sup>48</sup> Desilicization or dealumination will result in a larger pore structure, as shown in Fig. 5. Based on the results, it can be concluded that the acid modification succeeded in removing the Al element in ZSM-5, while the alkali modification successfully removed the Si element in ZSM-5.

Fig. 3 shows SEM images of ZSM-5, ZSM-5-H, ZSM-5-OH and ZSM-5-H-OH zeolites. We can observe that the unmodified ZSM-5 has a smooth morphological surface and a highly ordered structure with only a small number of pores, demonstrating

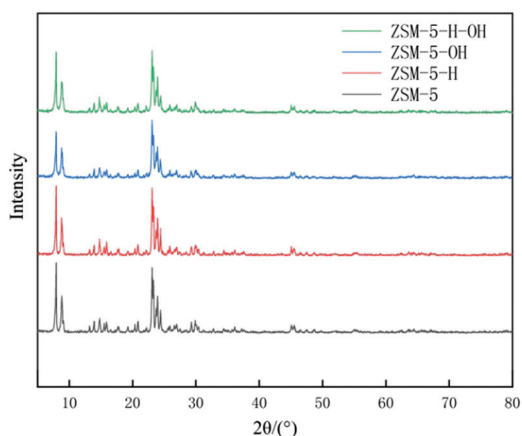
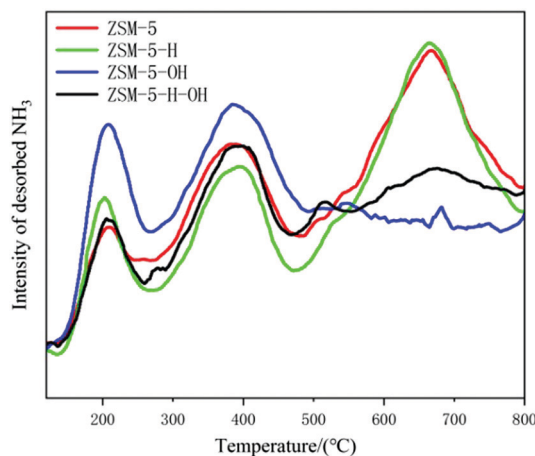


Fig. 1 XRD patterns of HZSM-5 zeolites before and after treatment.

Fig. 2 NH<sub>3</sub>-TPD profiles of parent and modified ZSM-5.

the high crystallinity of ZSM-5 (Fig. 1). The acid-modified ZSM-5 morphology has undergone some changes, no longer a regular rectangular structure, and the pores are slightly increased (Fig. 3b). Although the alkali-modified ZSM-5 still retains the rectangular shape, many faults and voids have appeared inside. This is consistent with what other researchers have observed.<sup>49,50</sup> The acid-base co-modified ZSM-5 not only changed its morphology, but also showed many pores inside. The acid-alkali co-modified ZSM-5 has changed its appearance in addition to having more pores. This indicates that the modification by acid and alkali not only causes a mesoporous structure in ZSM-5, but also changes the morphology of ZSM-5.

Fig. 4 shows the N<sub>2</sub> adsorption isotherms and pore size distribution of ZSM-5 and modified ZSM-5. As shown in Fig. 4A, unmodified ZSM-5 and acid-modified ZSM-5 exhibited a type I adsorption isotherm, indicating a microporous structure. Comparing the two adsorption isotherms, we can find that the adsorption isotherm of acid-modified ZSM-5 has no significant change compared to the adsorption isotherm of unmodified ZSM-5, indicating that the modification by acid had no significant effect on the pore structure of ZSM-5. The alkali-modified ZSM-5 and the acid-alkali co-modified ZSM-5 showed a type IV adsorption isotherm, and a hysteresis loop appeared, which was typically associated with the emptying and the filling of mesopores, indicating that a mesoporous structure appeared in the pores of ZSM-5. This is consistent with the observations of TEM. The process of alkali modification is shown in Fig. 5, in which a larger pore structure and a larger specific surface area are obtained by removing the silicon element in ZSM-5. As shown in Fig. 4B, it can be found that the mesoporous pore size distribution of all the ZSM-5 samples is mainly concentrated at 3.5 nm, and the 3.5 nm mesoporous distributions of the alkali-modified ZSM-5 and the acid-alkali co-modified ZSM-5 are more visible. As shown in Table 4, the BET surface area, external surface area, and pore volume of the ZSM-5 and the acid-alkali co-modified ZSM-5 were significantly increased, while the microporous area was significantly reduced, which was attributable to the ZSM-5 part of the microporous structure in the channel being converted to a mesoporous structure.

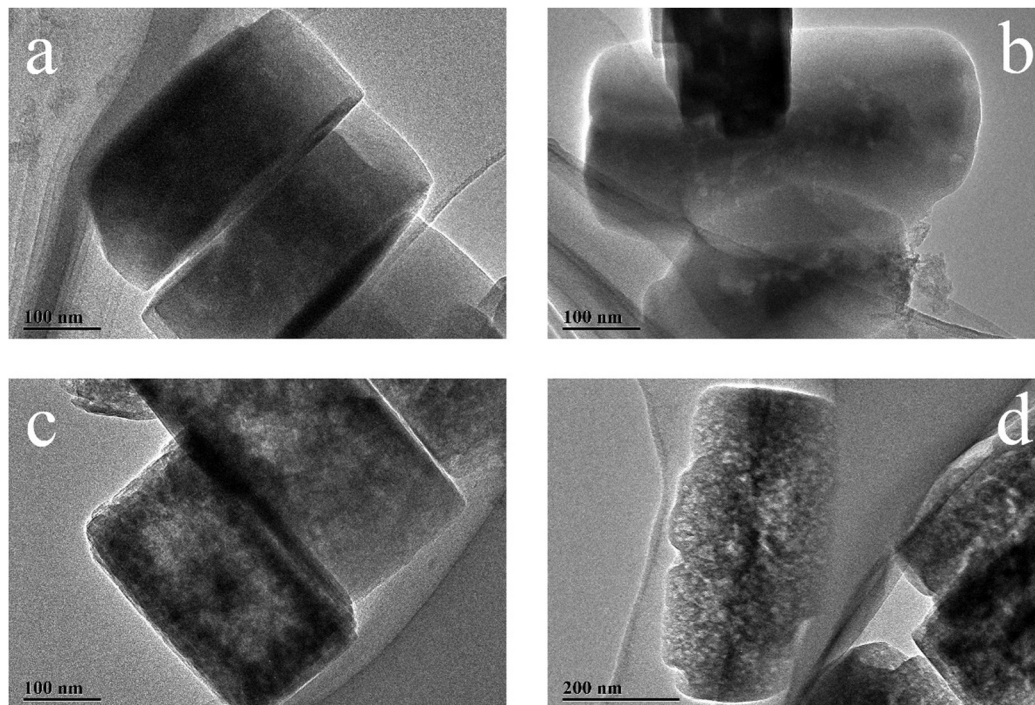


Fig. 3 TEM images before and after modification of ZSM-5: (a) ZSM-5, (b) ZSM-5-H, (c) ZSM-5-OH and (d) ZSM-5-H-OH.

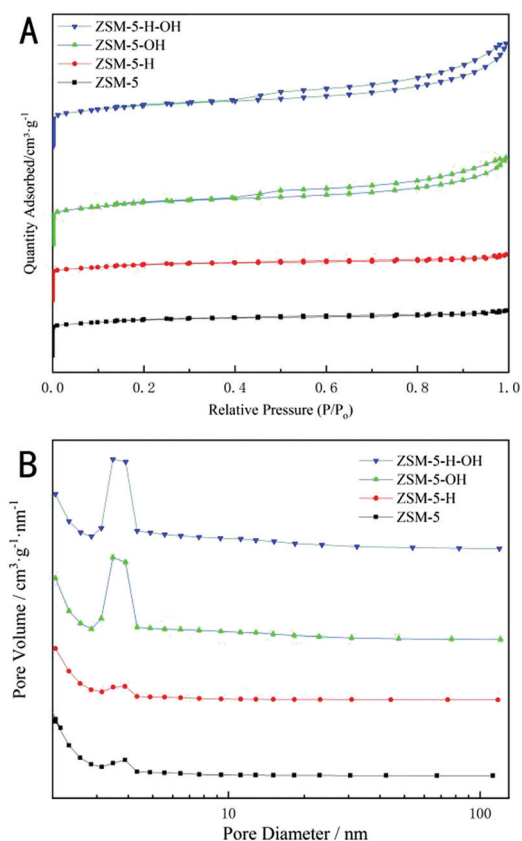


Fig. 4 (A)  $N_2$  adsorption and desorption isotherms and (B) BJH pore size distributions for different ZSM-5 samples.

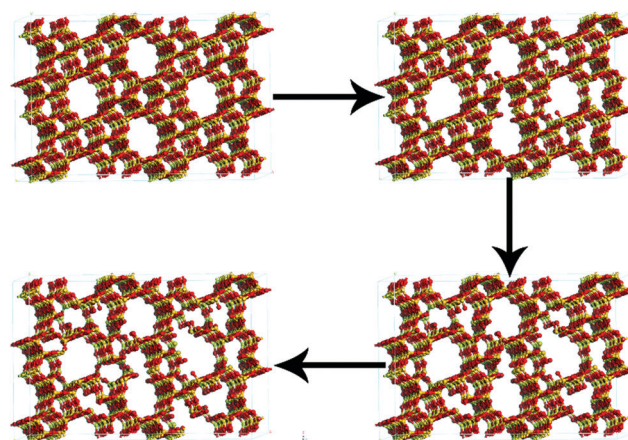


Fig. 5 ZSM-5 modification process diagram.

The acid-modified ZSM-5 did not change significantly compared to the unmodified ZSM-5.

### 3.2 Catalytic performance

ZSM-5 and modified ZSM-5 samples were evaluated in the alkylation reaction of benzene with synthesis gas, and the catalytic performance is shown in Table 4 and Fig. 6. The data in Table 4 and Fig. 6 are the average of multiple experiments, where the data for xylene refer to the sum of all isomers of xylene. We have found that although acid modification can increase the conversion of CO in the reaction, the selectivity to various aromatics is almost reduced.<sup>51</sup> In this reaction, the reactants CO and  $H_2$  produced methanol under the catalysis of Cu/ZnO/ $Al_2O_3$ , and then the methanol entered the pores of

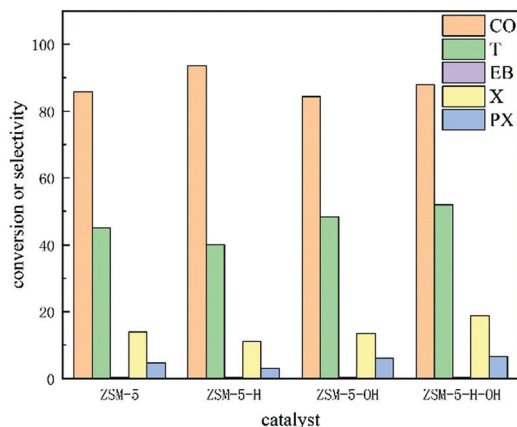


Fig. 6 Catalytic performance of different zeolites in benzene alkylation with methanol.

ZSM-5 and was adsorbed on the acidic sites, and alkylated benzene to form aromatic hydrocarbons (Fig. 7). The step of methanol to aromatics is the most critical. In this step, the MTO reaction is one of the main side reactions in which methanol is first dehydrated to dimethyl ether (DME), and the equilibrium mixture formed includes methanol, dimethyl ether and water, and then converted into light olefins. The olefins are converted to alkanes, aromatics, naphthenes and higher olefins by hydrogen transfer, alkylation and polycondensation. According to relevant literature reports, strong acid sites are conducive to the occurrence of MTO reactions.<sup>49,52</sup> We can find from Fig. 2 and Table 1 that the acid-modified ZSM-5 has increased acid sites compared to the unmodified ZSM-5, thereby increasing the MTO side reaction. At the same time, we can find from Table 3 and Fig. 3 that the pores of the acid-modified ZSM-5 did not increase significantly and did not have an increased

Table 3 The porosity properties for ZSM-5 before and after modification

Catalysts	Conversion/%	Selectivity/%			
		Toluene	Ethylbenzene	Xylene	<i>p</i> -Xylene
ZSM-5	85.8	45.1	0.3	13.8	4.6
ZSM-5-H	93.6	40.1	0.3	11.0	3.1
ZSM-5-OH	84.4	48.3	0.3	13.5	6.1
ZSM-5-H-OH	88.1	51.9	0.3	18.7	6.6

mesoporous structure. Therefore, the selectivity to aromatic hydrocarbons has decreased. It can be seen from Table S1 (ESI<sup>†</sup>) that Cu/ZnO/Al<sub>2</sub>O<sub>3</sub> only acts on the reaction of syngas to methanol, and has no effect on the reaction of methanol to aromatics, while ZSM-5 only acts on the reaction of methanol to aromatics, and has no effect on the reaction of syngas to methanol.

As shown in Fig. 6, the alkali-modified ZSM-5 has a higher selectivity than the unmodified ZSM-5 catalyst. We can see from Fig. 2 and Table 1 that the alkali-modified ZSM-5 is significantly reduced compared with ZSM-5 which is modified by acid and base, and the unmodified ZSM-5, so that the strong acid sites are greatly reduced, thus effectively inhibiting the side reaction of MTO. From the SEM image, we can see that this is due to the channels in the alkali-modified ZSM-5 catalyst, which provide a larger reaction area for the reactants to enter the active site. Furthermore, due to the effects of acid leaching, ZSM-5-H-OH showed better activity than ZSM-5-OH, resulting in more active site exposure and improved accessibility of the zeolite pores. From Table 3 and Fig. 3, we can also find that the specific surface area and pore volume of ZSM-5 modified by alkali modification and acid-base increase, while increasing the mesoporous structure. On the other hand, the selectivity to xylene has also been significantly improved, indicating that the

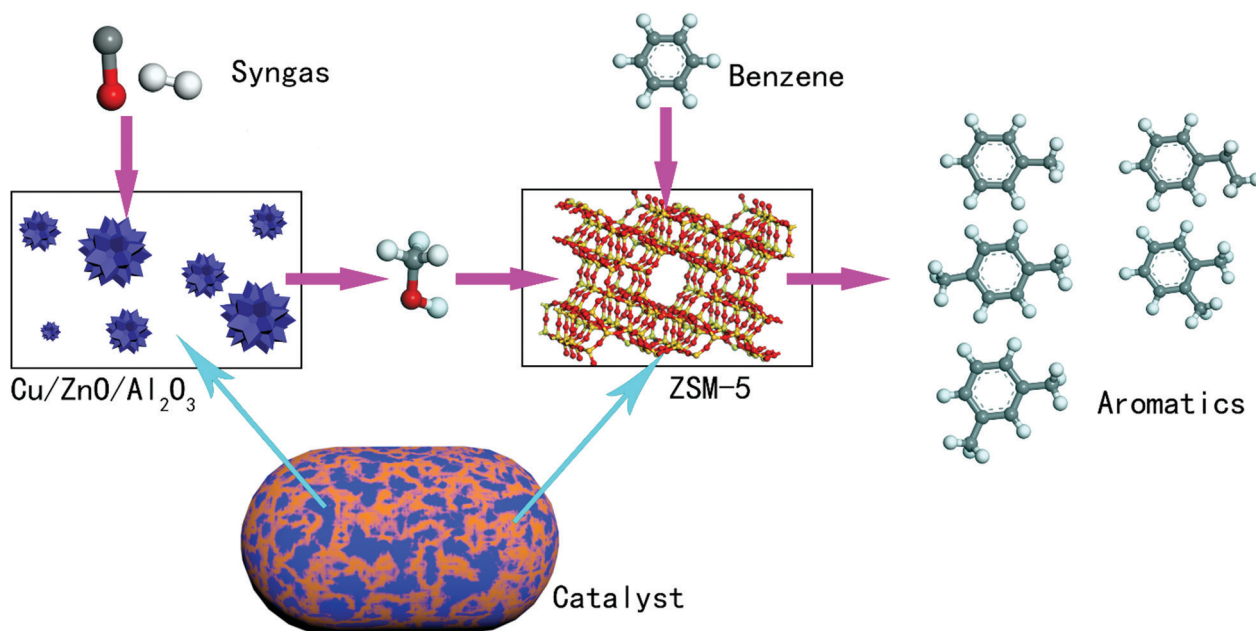


Fig. 7 Process for syngas and benzene to form aromatic hydrocarbons.

**Table 4** Catalytic performance of different zeolites in benzene alkylation with methanol

Samples	Surface area (m <sup>2</sup> g <sup>-1</sup> )			Pore volume (cm <sup>3</sup> g <sup>-1</sup> )	
	S <sub>BET</sub>	S <sub>ext/mes</sub>	S <sub>micro</sub>	V <sub>mesopore</sub>	V <sub>micro</sub>
ZSM-5	433.7	140.8	292.9	0.119	0.229
ZSM-5-H	431	135.9	295.1	0.12	0.233
ZSM-5-OH	487.8	240.5	247.2	0.103	0.433
ZSM-5-H-OH	489.9	247.8	242.1	0.103	0.52

presence of mesopores promotes the diffusion of large amounts of aromatics in the reaction.<sup>18,52</sup>

Ethylbenzene in the product is formed by alkylation of ethylene and benzene. Ethylene is produced by the Fischer–Tropsch synthesis of ethanol, and the composite catalyst of Cu/ZnO/Al<sub>2</sub>O<sub>3</sub> and ZSM-5 is not suitable as a Fischer–Tropsch synthesis catalyst.<sup>53</sup> Therefore, it is difficult for methanol to form ethylene, and therefore, only a small amount of toluene is produced in the product. This indicates that this experiment can be detrimental to the occurrence of the Fischer–Tropsch synthesis reaction, thereby reducing many side reactions related to olefins. The selectivity of ZSM-5, to toluene, xylene and *p*-xylene, is greatly improved by modification by acid and alkali. From the TEM image, we can see that ZSM-5-H-OH, compared with ZSM-5-OH, has more pores, which is more conducive to the diffusion of toluene and xylene. In summary, acid-alkali co-modified ZSM-5 significantly improves selectivity increase the catalytic activity and product selectivity of alkylation of benzene with methanol.

## 4. Conclusions

In summary, a ZSM-5 molecular sieve was successfully treated by acid modification, alkali modification or an acid-alkali method. The TEM images showed that a modified ZSM-5 appeared. It can be found that the pores of ZSM-5 modified by acid and alkali are the most obvious. The XRD patterns showed almost no change in the skeleton structure of the modified ZSM-5. It can be seen from the data of ICP that the acid-modified ZSM-5 silicon–aluminum ratio is larger, the alkali-modified ZSM-5 silicon–aluminum ratio is changed, and the acid-alkali co-modified ZSM-5 silicon–aluminum ratio is slightly smaller. From the NH<sub>3</sub>-TPD patterns, it can be found that the amount of modified ZSM-5 acid sites has changed greatly, especially the strong acid positions of ZSM-5 modified by alkali modification and acid-alkali co-modification have been greatly reduced. From the BET analysis, we can find that the surface area and pore volume of the alkali-modified ZSM-5 and the acid-alkali co-modified ZSM-5 are significantly increased, and more mesoporous structures appear, while in the acid-modified ZSM-5 the changes are not obvious. From the activity test of the catalyst, we can see that the conversion by the acid-modified ZSM-5 is improved, but the selectivity to the aromatic hydrocarbons is decreased, while the selectivity of the alkali-modified ZSM-5 to the aromatic hydrocarbons is improved, and that of the acid-alkali-modified ZSM-5 is normal.

The acid-alkali co-modified ZSM-5 not only has an improved conversion rate, but also a significant increase in the selectivity to aromatic hydrocarbons, and the amount of industrially required *para*-xylene is also increased. Compared to Zhao<sup>54</sup> and Bai's<sup>55</sup> research, this catalyst not only has higher conversion and selectivity, but also the reaction can be carried out at lower pressures and temperatures. The acid-alkali co-modified ZSM-5 has formed many mesoporous structures, which improved its mass transfer ability and is the main reason for the improvement of selectivity to aromatics.

## Conflicts of interest

The authors declare no competing financial interest.

## Acknowledgements

This research was funded by the Natural Science Foundation of China, grant number 21706178, and 21978189; Natural Science Foundation of Shanxi Province, grant number 201801D221074, and 201801D121058; China Postdoctoral Science Foundation 2019M651079. The authors also gratefully acknowledge the support and guidance of teachers of the 508 groups from Institute of Coal Chemistry, Chinese Academy of Sciences.

## Notes and references

- 1 A. M. Niziolek, O. Onel and C. A. Floudas, *AIChE J.*, 2016, **62**, 1531–1556.
- 2 Y. Zhao, W. Tan, H. Wu, A. Zhang, M. Liu, G. Li, X. Wang, C. Song and X. Guo, *Catal. Today*, 2011, **160**, 179–183.
- 3 S. M. Lee, W. J. Choi, K. Hwang, J. H. Kim and J. Y. Lee, *Macromol. Res.*, 2014, **22**, 481–486.
- 4 X. Wang, J. Xu, G. Qi, B. Li and C. Wang, *J. Phys. Chem. C*, 2013, **117**, 4018–4023.
- 5 H. Hu, J. Lyu, Q. Wang, Q. Zhang, J. Cen and X. Li, *RSC Adv.*, 2015, **5**, 32679–32684.
- 6 L. Shi, G. Yang, K. Tao, Y. Yoneyama, Y. Tan and N. Tsubaki, *Acc. Chem. Res.*, 2013, **46**, 1838–1847.
- 7 G. Centi, E. A. Quadrelli and S. Perathoner, *Energy Environ. Sci.*, 2013, **6**, 1711–1731.
- 8 Y. Tang, Y. Li, V. Fung, D. Jiang, W. Huang, S. Zhang, Y. Iwasawa, T. Sakata, L. Nguyen, X. Zhang, A. I. Frenkel and F. Tao, *Nat. Commun.*, 2018, **9**, 1231.
- 9 N. M. Tukur and S. Al-Khattaf, *Chem. Eng. J.*, 2011, **166**, 348–357.
- 10 K. Cheng, W. Zhou, J. Kang, S. He, S. Shi, Q. Zhang, Y. Pan, W. Wu and W. Ye, *Chem*, 2017, **3**, 334–347.
- 11 V. M. Lebarbier Dagle, R. A. Dagle, J. Li, C. Deshmane, C. E. Taylor, X. Bao and Y. Wang, *Ind. Eng. Chem. Res.*, 2014, **53**, 13928–13934.
- 12 X. Niu, J. Gao, Q. Miao, M. Dong, G. Wang, W. Fan, Z. Qin and J. Wang, *Microporous Mesoporous Mater.*, 2014, **197**, 252–261.

- 13 C. Song, K. Liu, D. Zhang, S. Liu, X. Li, S. Xie and L. Xu, *Appl. Catal., A*, 2014, **470**, 15–23.
- 14 K. Shen, W. Qian, N. Wang, C. Su and F. Wei, *J. Mater. Chem. A*, 2014, **2**, 19797–19808.
- 15 M. R. Gogate, *Pet. Sci. Technol.*, 2019, **3**, 671–678.
- 16 M. R. Gogate, *Pet. Sci. Technol.*, 2019, **37**, 603–610.
- 17 K. Cheng, B. Gu, X. Liu, J. Kang, Q. Zhang and Y. Wang, *Angew. Chem., Int. Ed.*, 2016, **55**, 4725–4728.
- 18 F. Jiao, J. Li, X. Pan, J. Xiao, H. Li, H. Ma, M. Wei, Y. Pan, Z. Zhou, M. Li, S. Miao, J. Li, Y. Zhu, D. Xiao, T. He, J. Yang, F. Qi, Q. Fu and X. Bao, *Science*, 2016, **351**, 1065–1068.
- 19 M. Li, L. Jiao, M. A. Nawaz, L. Cheng, C. Meng, T. Yang, M. Tariq and D. Liu, *Chem. Eng. Sci.*, 2019, **200**, 103–112.
- 20 Y. Bai, F. Yang, X. Liu, C. Liu and X. Zhu, *Catal. Lett.*, 2018, **148**, 3618–3627.
- 21 X. Zhao, F. Zeng, B. Zhao and H. Gu, *China Pet. Process. Petrochem. Technol.*, 2015, **17**, 31–38.
- 22 J. Kärger and D. Freude, *Chem. Eng. Technol.*, 2002, **25**, 769–778.
- 23 J. H. Kim, T. Kunieda and M. Niwa, *J. Catal.*, 1998, **173**, 433–439.
- 24 J. Perez-Ramirez, C. H. Christensen, K. Egeblad, C. H. Christensen and J. C. Groen, *Chem. Soc. Rev.*, 2008, **37**, 2530–2542.
- 25 C. H. Christensen, K. Johannsen, I. Schmidt and C. H. Christensen, *J. Am. Chem. Soc.*, 2003, **125**, 13370–13371.
- 26 Q. Che, M. Yang, X. Wang, Q. Yang, Y. Chen, X. Chen, W. Chen, J. Hu, K. Zeng, H. Yang and H. Chen, *Bioresour. Technol.*, 2019, **289**, 121729.
- 27 W. Fan, M. A. Snyder, S. Kumar, P. S. Lee, W. C. Yoo, A. V. McCormick, R. L. Penn, A. Stein and M. Tsapatsis, *Nat. Mater.*, 2008, **7**, 984.
- 28 C. J. H. Jacobsen, C. Madsen, J. Houzvicka, I. Schmidt and A. Carlsson, *J. Am. Chem. Soc.*, 2000, **122**, 7116–7117.
- 29 D. H. Park, S. S. Kim, H. Wang, T. J. Pinnavaia, M. C. Papapetrou, A. A. Lappas and K. S. Triantafyllidis, *Angew. Chem., Int. Ed.*, 2009, **48**, 7645–7648.
- 30 J. C. Groen, J. A. Moulijn and J. Pérez-Ramírez, *J. Mater. Chem.*, 2006, **16**, 2121–2131.
- 31 K. Gao, S. Li, L. Wang and W. Wang, *RSC Adv.*, 2015, **5**, 45098–45105.
- 32 D. Verboekend and J. Pérez-Ramírez, *Catal. Sci. Technol.*, 2011, **1**, 879–890.
- 33 W. Xiao, F. Wang and G. Xiao, *RSC Adv.*, 2015, **5**, 63697–63704.
- 34 T. Pan, Z. Wu and A. C. K. Yip, *Catalysts*, 2019, **9**, 274.
- 35 M. Bjørgen, F. Joensen, M. S. Holm, U. Olsbye, K. P. Lillerud and S. Svelle, *Appl. Catal., A*, 2008, **345**, 43–50.
- 36 J. Li, X. Y. Li, G. Q. Zhou, W. Wang, C. W. Wang, S. Komarneni and Y. J. Wang, *Appl. Catal., A*, 2014, **470**, 115–122.
- 37 T. L. D. Lu, *Doc. Praehistorica*, 2012, **39**, 111–136.
- 38 F. Meng, Y. Wang and S. Wang, *RSC Adv.*, 2016, **6**, 58586–58593.
- 39 H. Hu, Q. Zhang, J. Cen and X. Li, *Catal. Commun.*, 2014, **57**, 129–133.
- 40 T. Li, J. Ihli, J. T. C. Wennmacher, F. Krumeich and J. A. van Bokhoven, *J. Phys. Chem. C*, 2019, **123**, 8793–8801.
- 41 F. Meng, Y. Wang and S. Wang, *RSC Adv.*, 2016, **6**, 58586–58593.
- 42 H. Mochizuki, T. Yokoi, H. Imai, S. Namba, J. N. Kondo and T. Tatsumi, *Appl. Catal., A*, 2012, **449**, 188–197.
- 43 Q. Wang, W. Han, H. Hu, J. Lyu, X. Xu, Q. Zhang, H. Wang and X. Li, *Chin. J. Chem. Eng.*, 2017, **25**, 1777–1783.
- 44 Z. Di, C. Yang, X. Jiao, J. Li, J. Wu and D. Zhang, *Fuel*, 2013, **104**, 878–881.
- 45 Y. Wei, P. E. de Jongh, M. L. M. Bonati, D. J. Law, G. J. Sunley and K. P. de Jonga, *Appl. Catal., A*, 2015, **504**, 211–219.
- 46 L. Su, L. Liu, J. Zhuang, H. Wang, Y. Li, W. Shen, Y. Xu and X. Bao, *Catal. Lett.*, 2003, **91**, 155–167.
- 47 X. Wang, J. Zhang, T. Zhang, H. Xiao, F. Song, Y. Han and Y. Tan, *RSC Adv.*, 2016, **6**, 23428–23437.
- 48 K. Sasowska, A. Wach, Z. Olejniczak, P. Kustrowski and J. Datka, *Microporous Mesoporous Mater.*, 2013, **167**, 82–88.
- 49 H. Mochizuki, T. Yokoi, H. Imai, S. Namba and J. N. Kondo, *Appl. Catal., A*, 2012, **449**, 188–197.
- 50 H. Zhang, Y. Ma, K. Song, Y. Zhang and Y. Tang, *J. Catal.*, 2013, **302**, 115–125.
- 51 T. Hui, W. Jun, R. E. N. Xiaoqian and C. Demin, *Chin. J. Chem. Eng.*, 2011, **19**, 292–298.
- 52 M. D. González, Y. Cesteros and P. Salagre, *Microporous Mesoporous Mater.*, 2011, **144**, 162–170.
- 53 S. Kasipandi and J. W. Bae, *Adv. Mater.*, 2019, 1803390.
- 54 X. Zhao, F. Zeng, B. Zhao and H. Gu, *China Pet. Process. Petrochem. Technol.*, 2015, **17**, 31–38.
- 55 Y. Bai, F. Yang, X. Liu, C. Liu and X. Zhu, *Catal. Lett.*, 2018, **148**, 3618–3627.